




## Shot-noise-suppressing quantum nonlinearity in the vacuum-field-induced photon-photon interaction

Jiang-Shan Tang <sup>1,2</sup>, Lei Tang,<sup>1</sup> Zhi-Xiang Li,<sup>1</sup> Ya-Ping Ruan,<sup>1</sup> Han Zhang <sup>2</sup> and Keyu Xia <sup>1,3,\*</sup>

<sup>1</sup>*College of Engineering and Applied Sciences, National Laboratory of Solid State Microstructures, and Collaborative Innovation Center of Advanced Microstructures, Nanjing University, Nanjing 210023, China*

<sup>2</sup>*School of Physics, Nanjing University, Nanjing 210023, China*

<sup>3</sup>*Jiangsu Key Laboratory of Artificial Functional Materials, Nanjing University, Nanjing 210023, China*



(Received 22 February 2022; accepted 20 December 2022; published 28 December 2022)

The shot noise in coherent control of a quantum system sets an ultimate precision limit in measurement and information processing. It is caused by the fundamental quantum fluctuation of the photon number of a coherent control field and thus is inevitable. By strongly coupling a two-level system to a quantum vacuum field, we propose an effective  $N$ -type four-level system. In such a configuration, the coupling of a conventional  $N$ -type system to a coherent control field is replaced by the quantum vacuum field. As a result, we can achieve a shot-noise-suppressing quantum nonlinearity, due to the vanishing fluctuation of photon number of the quantum vacuum field. The resulting photon blockade effect is only subject to the contribution from the probe field. Thus, it becomes shot-noise suppressing. Our work shows an advantage of a quantum vacuum protocol over a coherent-field protocol in manipulation of quantum systems and presents an opportunity to exploit the quantum vacuum field as a powerful tool in quantum information processing.

DOI: [10.1103/PhysRevA.106.062439](https://doi.org/10.1103/PhysRevA.106.062439)

### I. INTRODUCTION

The laser plays a key role in regulating quantum systems for quantum information processing [1]. However, the photon-number fluctuation is inevitable in a coherent light field. This shot-noise fluctuation typically has a Poisson distribution [2,3], leading to the so-called standard quantum limit in quantum simulation [4], quantum measurement [5,6], and imaging [7]. Although many schemes have been proposed to control quantum fluctuations [8,9], it is still very challenging to eliminate this intrinsic noise and then beat the standard quantum limit. In this work we exploit the quantum vacuum field to induce a shot-noise-suppressing quantum nonlinearity and to circumvent the limitation of photon-number fluctuation related to the coherent control field in quantum information processing.

The quantum vacuum field is a fundamental concept in quantum physics. To explain the spontaneous photon emission, Dirac proposed that an excited quantum emitter (QE) can transfer energy by emitting a photon into a quantum vacuum field unoccupied electromagnetic mode [10], breaking the common perception of a quantum vacuum as the absence of everything [11]. Due to such a counterintuitive picture, the nature of quantum vacuum fields quickly draws intensive attention [12–14]. The interest ranges from the basic science to potential applications of technology [11] such as vacuum-field detection [15,16], Casimir effect [17], Lamb spectral shifts [2], and vacuum-induced phonon heat transfer [18].

The interaction of a continuum-mode light field with a QE is usually weak in free space, resulting in imperceptible effects of the vacuum-field coupling. In space confined by an optical cavity, the intracavity matter strongly couples to the discrete optical modes of the cavity, even in the quantum vacuum state without any photons [11]. Thus, the quantum properties of a QE can be greatly modified with an optical cavity [19,20]. This cavity-enhanced light-QE interaction gives birth to cavity quantum electrodynamics (QED) [2,21]. The quantum vacuum-induced coupling (VIC) of QEs and an optical cavity can generate a photon-photon interaction without the use of an external light field. It also leads to many exotic physical phenomena, including vacuum Rabi splitting in a two-level QE [12,22–25] and vacuum-induced transparency in a three-level quantum system [13].

Conventionally, the nonlinear interaction between photons is very weak. A cavity QED system with an  $N$ -type four-level QE controlled by a coherent field can be used to achieve a strong photon-photon interaction [26,27]. Compared to a cavity QED system with a two-level QE, this  $N$ -type cavity QED system has the merits of a giant quantum nonlinearity of photons. Therefore, it promises many important applications in quantum information technologies such as quantum phase gates [28–30] and the single-photon extraction via the photon blockade effect [31]. The concept of photon blockade has been extended to the phonon domain recently by creating a phononic  $N$ -type quantum system with the VIC [32]. Nonetheless, the advantage of the quantum vacuum field as a resource for quantum information processing has barely been addressed.

Here we propose a vacuum-induced  $N$ -type system superior to a coherent-field-controlled  $N$ -type system in generating

\*keyu.xia@nju.edu.cn

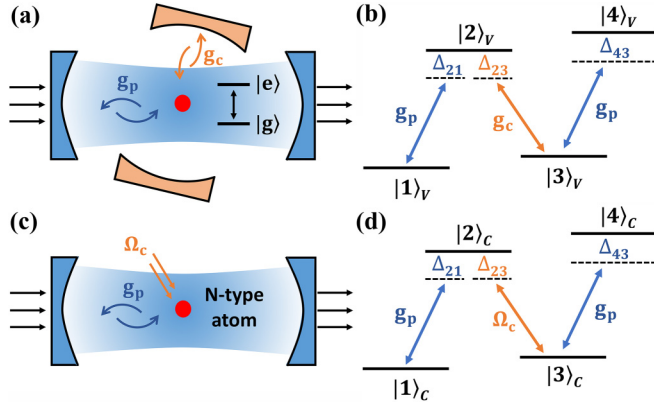


FIG. 1. Schematic diagram of the  $N$ -type VIC and CFC configurations. (a) Schematic of the VIC configuration consisting of a two-level QE, an auxiliary cavity composed of upper and lower cavity mirrors (yellow), and a probe cavity composed of left and right cavity mirrors (blue). (b) Level diagram of the vacuum-induced  $N$ -type system. (c) Schematic of the CFC configuration, containing an  $N$ -type QE and a probe cavity. (d) Level diagram of the coherent-field-controlled  $N$ -type system.

quantum nonlinearity for photon blockade. By modeling the classical coherent field as a coherently driven cavity, we show a considerably large shot noise in the coherent-field-coupling (CFC) protocol. In contrast, the shot noise caused by the coherent control field disappears in the VIC protocol, achieving a shot-noise-suppressing Kerr photonic nonlinearity.

## II. SYSTEM AND MODEL

The VIC configuration, as shown in Fig. 1(a), consists of a two-level QE with a resonance frequency  $\omega_e$ , an auxiliary cavity, and a probe cavity. The auxiliary cavity  $\hat{d}$  and the probe cavity  $\hat{a}$  couple to the two-level QE with strengths  $g_c$  and  $g_p$ , respectively. We consider that the auxiliary cavity is made from two perfect mirrors such that only the intrinsic loss  $\kappa_{d,i}$  should be taken into account in the decay. A weak coherent probe field with amplitude  $\alpha_{\text{in}}$  is incident to the probe cavity from the left input port. We are interested in the transmitted field to the right output port. The probe cavity has three main decay channels [33]:  $\kappa_{p,e1}$  for the input port,  $\kappa_{p,i}$  for the intrinsic decay, and  $\kappa_{p,e2}$  for the output port. The total decay rate is  $\kappa_p = \kappa_{p,e1} + \kappa_{p,i} + \kappa_{p,e2}$ . In experiments, the intrinsic loss  $\kappa_{d,i}$  can be far less than  $\kappa_p$  [21,34]. In the case of a weak probe and  $g_p \ll g_c$ , the quantum vacuum state with zero photons is mostly populated in the auxiliary cavity. Thus, it is reasonable to truncate the cavity mode  $\hat{d}$  up to the first excited Fock state  $|1_d\rangle$ .

The subsystem of the two-level QE and the auxiliary cavity can be modeled as a four-level system with  $|1\rangle_V = |g, 0_d\rangle$  for the vacuum state,  $|2\rangle_V = |e, 0_d\rangle$ ,  $|3\rangle_V = |g, 1_d\rangle$ , and  $|4\rangle_V = |e, 1_d\rangle$  [32], as shown in Fig. 1(b). Taking the ground state  $|1\rangle_V$  as a reference, the energies of the remaining three states are  $\omega_e$ ,  $\omega_c$ , and  $\omega_e + \omega_c$ . In this case, we create an  $N$ -type four-level quantum system with the VIC. In such an equivalent configuration, the quantum vacuum field drives the transition  $|2\rangle_V \leftrightarrow |3\rangle_V$  and the probe cavity mode couples to the transitions  $|1\rangle_V \leftrightarrow |2\rangle_V$  and  $|3\rangle_V \leftrightarrow |4\rangle_V$ . It is worth noting

that this VIC configuration allows an on-chip platform of a two-level superconducting qubit coupling to a microwave resonator [35].

The loss of the auxiliary cavity mode  $\hat{d}$  causes the state  $|3\rangle_V$  ( $|4\rangle_V$ ) to decay to the state  $|1\rangle_V$  ( $|2\rangle_V$ ) with a rate  $\gamma_{31} = 2\kappa_{d,i}$  ( $\gamma_{42} = 2\kappa_{d,i}$ ). The two-level QE has a relaxation rate  $\gamma$ . Because of this relaxation, the state  $|2\rangle_V$  ( $|4\rangle_V$ ) decays to the state  $|1\rangle_V$  ( $|3\rangle_V$ ) with a rate  $\gamma_{21} = \gamma$  ( $\gamma_{43} = \gamma$ ). We find that there is no decay channel between states  $|2\rangle_V$  and  $|3\rangle_V$  (see Appendix A), that is,  $\gamma_{23} = 0$ . The transition between  $|2\rangle_V$  and  $|3\rangle_V$  results from the interaction of the two-level QE with the quantum vacuum field mode in the auxiliary cavity and thus replacing the conventional decoherence mechanism.

In the basis of  $\{|1\rangle_V, |2\rangle_V, |3\rangle_V, |4\rangle_V\}$  and the frame rotating at frequency  $\omega_a$ , the system Hamiltonian of the VIC configuration is given by ( $\hbar = 1$ )

$$\hat{H}_{\text{VIC}} = \hat{H}_{\text{VIC}}^S + \hat{H}_{\text{VIC}}^P, \quad (1a)$$

$$\hat{H}_{\text{VIC}}^S = \Delta_{21}\hat{\sigma}_{22} + (\Delta_{21} - \Delta_{23})\hat{\sigma}_{33} + (\Delta_{43} + \Delta_{21} - \Delta_{23})\hat{\sigma}_{44} + [g_p(\hat{a}^\dagger\hat{\sigma}_{12} + \hat{a}\hat{\sigma}_{34}) + g_c\hat{\sigma}_{23} + \text{H.c.}], \quad (1b)$$

$$\hat{H}_{\text{VIC}}^P = i\sqrt{2\kappa_{p,e1}}\alpha_{\text{in}}(\hat{a}^\dagger e^{-i\Delta_p t} - \hat{a}e^{i\Delta_p t}), \quad (1c)$$

where  $\Delta_{21} = \Delta_{43} = \omega_e - \omega_a$  ( $\Delta_{23} = \omega_e - \omega_c$ ) is the detuning between the two-level QE and the probe cavity mode (the auxiliary cavity mode) and  $\Delta_p = \omega_p - \omega_a$  is the probe-field detuning. The operator  $\hat{\sigma}_{mn} = |m\rangle\langle n|_V$  ( $n, m = 1, 2, 3, 4$ ) stands for the transition of the  $N$ -type system. The interaction Hamiltonian is described by Eq. (1b) and the last term  $\hat{H}_{\text{VIC}}^P$  represents the driving Hamiltonian related to the probe field.

We now describe the CFC configuration shown in Fig. 1(c). Unlike the VIC-based  $N$ -type system, a natural  $N$ -type atom, such as a rubidium atom, can be placed in a Fabry-Pérot optical cavity to achieve a strong photon-photon interaction [36–39]. A coherent control field directly drives the transition  $|2\rangle_C \leftrightarrow |3\rangle_C$  with a Rabi frequency  $\Omega_c$  [see Fig. 1(d)]. We use the same probe setup as the VIC protocol. The system Hamiltonian of this CFC configuration reads

$$\hat{H}'_{\text{CFC}} = \hat{H}'_{\text{CFC}}^S + \hat{H}'_{\text{CFC}}^P, \quad (2a)$$

$$\hat{H}'_{\text{CFC}}^S = \Delta_{21}\hat{\sigma}_{22} + (\Delta_{21} - \Delta_{23})\hat{\sigma}_{33} + (\Delta_{43} + \Delta_{21} - \Delta_{23})\hat{\sigma}_{44} + [g_p(\hat{a}^\dagger\hat{\sigma}_{12} + \hat{a}\hat{\sigma}_{34}) + \Omega_c\hat{\sigma}_{23} + \text{H.c.}], \quad (2b)$$

$$\hat{H}'_{\text{CFC}}^P = i\sqrt{2\kappa_{p,e1}}\alpha_{\text{in}}(\hat{a}^\dagger e^{-i\Delta_p t} - \hat{a}e^{i\Delta_p t}), \quad (2c)$$

where  $\hat{\sigma}_{mn} = |m\rangle\langle n|_C$  ( $m, n = 1, 2, 3, 4$ ) defines the transition operator for the four-level atom. Notably, due to the decoherence mechanism of natural  $N$ -type atomic energy levels, we retain the decay from  $|2\rangle_C$  to  $|3\rangle_C$ . In addition, to compare with the VIC protocol, we consider the same decay rates for the  $N$ -type quantum system and the probe cavity.

Comparing Eqs. (1) and (2) and two-level diagrams, we can see that the two configurations are different only in the coupling to the transition  $|2\rangle \leftrightarrow |3\rangle$ . In the VIC configuration, this coupling is caused by the quantum vacuum field of the auxiliary cavity driving the two-level QE. The coupling strength is a pure number  $g_c$  in a practical experimental implementation of this VIC configuration [35]. In contrast, the coupling  $\Omega_c$  is the coherent control field driving the real transition  $|2\rangle \leftrightarrow |3\rangle$  of a natural  $N$ -type atom. In conventional

treatment, the coupling strength  $\Omega_c$  in the CFC configuration is treated as a number without fluctuation [2]. This treatment causes the Hamiltonian (2) to fail to reflect the photon-number fluctuation of the coherent control field. Indeed, it is valid when the coherent field is strong enough.

In a theoretical model of the coherent-field driving of the atom, the coherent control field  $\Omega_c$  can be replaced by an open-environment pseudocavity mode  $\hat{c}$  with a total decay rate  $\kappa_c$ . A new coherent field  $\xi$  resonantly excites the pseudocavity mode to a coherent state  $|\alpha\rangle$ , which generates an equivalent driving as  $\Omega_c$  to the atom. In this case, we have  $\Omega_c = \alpha g'_c$ , where  $g'_c$  is the mean single-photon coupling strength. In doing so, the quantum fluctuation of the coherent control field in experiment, corresponding to the shot noise, can be taken into account in the model. The Hamiltonian describing this equivalent pseudocavity QED system can be written as

$$\hat{H}_{\text{CFC}} = \hat{H}_{\text{CFC}}^S + \hat{H}_{\text{CFC}}^P, \quad (3a)$$

$$\begin{aligned} \hat{H}_{\text{CFC}}^S &= \Delta_{21}\hat{\sigma}_{22} + (\Delta_{21} - \Delta_{23})\hat{\sigma}_{33} + (\Delta_{43} + \Delta_{21} - \Delta_{23}) \\ &\quad \times \hat{\sigma}_{44} + [g_p(\hat{a}^\dagger\hat{\sigma}_{12} + \hat{a}^\dagger\hat{\sigma}_{34}) + g'_c\hat{\sigma}_{23}\hat{c} + h.c.] \\ &\quad + i\xi(\hat{c}^\dagger - \hat{c}), \end{aligned} \quad (3b)$$

$$\hat{H}_{\text{CFC}}^P = i\sqrt{2\kappa_{p,e1}}\alpha_{\text{in}}(\hat{a}^\dagger e^{-i\Delta_p t} - \hat{a}e^{i\Delta_p t}), \quad (3c)$$

where  $\hat{c}$  is the annihilation operator of the pseudocavity mode. The quantum-averaged photon number  $N_c$  of the pseudocavity field is proportional to the square of driving amplitude  $\xi$ , given by  $N_c = \langle \hat{c}^\dagger \hat{c} \rangle = \xi^2 / \kappa_c^2$ . The relation between  $\Omega_c$  and  $g'_c$  is  $\Omega_c = g'_c \sqrt{N_c}$ . We take  $\Omega_c = g_c$  to keep the coupling rates consistent in the two configurations.

Hereafter, we study the photon-number fluctuation of the CFC configuration based on this pseudocavity QED model. The VIC protocol, which makes full use of the quantum vacuum field in an auxiliary cavity interacting with a two-level QE, provides an effective approach to suppress the shot noise of the control field, while it is inevitable in the CFC protocol.

The dynamics of the quantum system with an observable operator  $\hat{O}$  is governed by the quantum master equation

$$\dot{\hat{O}}(t) = -i[\hat{O}(t), \hat{H}] + \mathcal{L}[\Gamma, \hat{A}]\hat{O}(t), \quad (4)$$

where the superoperator  $\mathcal{L}[\Gamma, \hat{A}]\hat{O}(t)$  describes the system dissipation and has the same form in the Heisenberg picture for both the VIC and CFC configurations as [33,40,41]

$$\mathcal{L}[\Gamma, \hat{A}]\hat{O}(t) = \Gamma(2\hat{A}^\dagger\hat{O}(t)\hat{A} - \hat{A}^\dagger\hat{A}\hat{O}(t) - \hat{O}(t)\hat{A}^\dagger\hat{A}), \quad (5)$$

with  $\Gamma = \{\kappa_p, \kappa_c, \gamma_{21}/2, \gamma_{23}/2, \gamma_{31}/2, \gamma_{43}/2, \gamma_{42}/2\}$  and  $\hat{A} = \{\hat{a}, \hat{c}, \hat{S}_{12}, \hat{S}_{32}, \hat{S}_{13}, \hat{S}_{34}, \hat{S}_{24}\}$  ( $\hat{S} = \hat{s}, \hat{\sigma}$ ). The motion of the systems can be accessed directly by numerically solving the quantum master equation [42].

### III. SHOT-NOISE-SUPPRESSING QUANTUM NONLINEARITY

We can also obtain the effective Hamiltonian by adiabatically eliminating the atomic operators in Eqs. (1). Using a perturbation approach to solve the master equation [2,31,32,43–45] (see Appendix A) and then applying an unitary transformation, defined by  $\hat{U} = \exp(i\Delta_p \hat{a}^\dagger \hat{a} t)$ , to the system with the probe in the VIC configuration, we obtain the

effective Hamiltonian

$$\begin{aligned} \hat{H}_{\text{VIC}}^{\text{eff}} &= (\Delta_p + \delta\omega_{\text{VIC}})\hat{a}^\dagger\hat{a} + \eta_{\text{VIC}}\hat{a}^\dagger\hat{a}^\dagger\hat{a}\hat{a} \\ &\quad + i\sqrt{2\kappa_{p,e1}}\alpha_{\text{in}}(\hat{a}^\dagger - \hat{a}), \end{aligned} \quad (6)$$

where  $\delta\omega_{\text{VIC}}$  is the linear frequency shift, which can be neglected in the case of two-photon resonance [37] in which  $\Delta_{21} = \Delta_{23}$ . The second term related to  $\eta_{\text{VIC}}$  describes the vacuum-induced quantum nonlinearity. Note that the nonlinearity strength  $\eta_{\text{VIC}}$  is a number in the VIC configuration. It is evaluated as

$$\eta_{\text{VIC}} = \frac{g_p^4(2\gamma_{31} + \gamma_{23})}{g_c^4\gamma_{31}(\gamma_{21} + \gamma_{23})} \left( \frac{1}{F} + \frac{1}{F^*} \right) \frac{\text{Im}(F)}{|F|^2}, \quad (7)$$

where  $F = \tilde{\gamma}_2/g_c^2 + 1/(\tilde{\gamma}_3 + g_p^2 N_a/\tilde{\gamma}_4)$ ,  $\tilde{\gamma}_2 = (\gamma_{21} + \gamma_{23})/2 + i\Delta_{21}$  ( $\gamma_{23} = 0$  in the VIC protocol),  $\tilde{\gamma}_3 = \gamma_{31}/2 + i(\Delta_{21} - \Delta_{23})$ ,  $\tilde{\gamma}_4 = (\gamma_{43} + \gamma_{42})/2 + i(\Delta_{43} + \Delta_{21} - \Delta_{23})$ , and  $N_a$  is the quantum-averaged photon number of the probe field. To a good approximation, we have  $N_a = |\alpha_{\text{in}}|^2/\kappa_p^2$  for  $\kappa_{p,e} \gg \kappa_{p,i}$ .

In the CFC configuration, the coherent control field has a photon-number fluctuation, i.e., subject to the shot noise. Such shot noise is difficult to assess using the conventional treatment of taking the coupling strength  $\Omega_c$  as a number. Thus, we use the pseudocavity QED model to analyze the effect of this quantum fluctuation of the coherent control field. We are interested in the pseudocavity mode  $\hat{c}$ . By adiabatically eliminating the atomic operators in Eq. (3), we get the effective Hamiltonian in the CFC configuration as

$$\begin{aligned} \hat{H}_{\text{CFC}}^{\text{eff}} &= (\Delta_p + \delta\omega_{\text{CFC}})\hat{a}^\dagger\hat{a} + \hat{\eta}_{\text{CFC}}\hat{a}^\dagger\hat{a}^\dagger\hat{a}\hat{a} \\ &\quad + i\sqrt{2\kappa_{p,e1}}\alpha_{\text{in}}(\hat{a}^\dagger - \hat{a}) \end{aligned} \quad (8)$$

and the corresponding quantum nonlinear coefficient

$$\hat{\eta}_{\text{CFC}} = \frac{g_p^4(2\gamma_{31} + \gamma_{23})}{g_c^4\langle \hat{c}^\dagger \hat{c} \rangle^2 \gamma_{31}(\gamma_{21} + \gamma_{23})} \left( \frac{1}{F} + \frac{1}{F^*} \right) \frac{\text{Im}(F)}{|F|^2}, \quad (9)$$

where the linear frequency shift  $\delta\omega_{\text{CFC}}$  is also negligible under the condition of two-photon resonance. The quantum nonlinear coefficient  $\hat{\eta}_{\text{CFC}}$  is no longer a pure number but an operator related to the photon-number operator  $\hat{c}^\dagger \hat{c}$ . Below we also refer to the photon-photon interaction coefficients  $\eta_{\text{VIC}}$  and  $\hat{\eta}_{\text{CFC}}$  as Kerr-type photonic nonlinearities.

We find that the nonlinearity  $\hat{\eta}_{\text{CFC}}$  depends on the photon number of the pseudocavity field [see the factor  $g_c^4\langle \hat{c}^\dagger \hat{c} \rangle^2$  in Eq. (9)]. The pseudocavity mode  $\hat{c}$  satisfies the relation  $\Omega_c = g'_c \sqrt{\langle \hat{c}^\dagger \hat{c} \rangle}$ , which leads to the fact that the mode  $\hat{c}$  cannot be in a vacuum state, thus avoiding the mathematical divergence of Eq. (9). In addition, from Eq. (9) it can be seen that the nonlinearity  $\hat{\eta}_{\text{CFC}}$  is inversely proportional to the photon number  $N_c$ . Under the condition that  $\Omega_c$  is strong enough to ensure the realization of electromagnetically induced transparency and an atomic coherent process, the smaller the photon number of the control field, the larger the nonlinearity. This point is confirmed both theoretically and experimentally [26,32,37,44,45].

In experimental measurement, the nonlinearity  $\hat{\eta}_{\text{CFC}}$  actually gets a number varying detection by detection, due to the random collapse of the quantum state. However, the photon-number fluctuation of the coherent control field introduces the shot noise to each measurement related to  $\hat{\eta}_{\text{CFC}}$ .

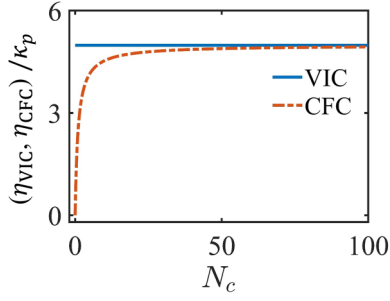


FIG. 2. Shot-noise-suppressing Kerr photonic nonlinearity. The red curve represents the nonlinear coefficient  $\eta_{\text{CFC}}$  of the CFC configuration, as a function of the average photon number  $N_c$ . The blue line is for the VIC configuration. The decay from  $|2\rangle$  to  $|3\rangle$  is  $\gamma_{23} = 0$  and  $\gamma_{23} = 0.1\kappa_p$  in the VIC and CFC configurations, respectively. The other parameters are  $\kappa_{p,i} = 0.2$ ,  $\kappa_{p,e1} = \kappa_{p,e2} = 0.4$ ,  $\kappa_p = 1$ ,  $\gamma_{21} = \gamma_{43} = 0.1\kappa_p$ ,  $\gamma_{42} = \gamma_{31} = 0.001\kappa_p$ ,  $\Delta_{21} = \Delta_{23} = \Delta_{43} = 0.5\kappa_p$ ,  $g_p = 15\kappa_p$ ,  $g_c = 60\kappa_p$ , and  $\Omega_c = 135\kappa_p$ .

In stark contrast,  $\eta_{\text{VIC}}$  in the VIC configuration is a pure number because the quantum vacuum field has zero fluctuation in the photon number. This means the uncertainty of the  $\eta_{\text{VIC}}$  measurement disappears, resulting in a shot-noise-suppressing Kerr nonlinearity.

The quantum-averaged Kerr nonlinearity of the CFC configuration,  $\eta_{\text{CFC}} = \langle \hat{\eta}_{\text{CFC}} \rangle$ , reflects the result of the average of multiple measurements of the system nonlinearity. As is well known, the photon-number fluctuation of a coherent field is proportional to the square root of the number of photons, that is,  $\Delta N_c = \sqrt{N_c}$ . Also, we have the relation  $\langle (\hat{\delta}^\dagger \hat{\delta})^2 \rangle = N_c^2 + \Delta N_c^2$  [2]. Therefore, we can rewrite the quantum-averaged nonlinear coefficient for the CFC configuration

$$\eta_{\text{CFC}} = \frac{\bar{\eta}_{\text{CFC}}}{1 + \Delta N_c^2 / N_c^2} = \frac{\bar{\eta}_{\text{CFC}}}{1 + 1/N_c}, \quad (10a)$$

$$\bar{\eta}_{\text{CFC}} = \frac{g_p^4 (2\gamma_{31} + \gamma_{23})}{\Omega_c^4 \gamma_{31} (\gamma_{21} + \gamma_{23})} \left( \frac{1}{F} + \frac{1}{F^*} \right) \frac{\text{Im}(F)}{|F|^2}. \quad (10b)$$

In what follows, to compare the two configurations, we take  $\bar{\eta}_{\text{CFC}} = \eta_{\text{VIC}}$  by adjusting the parameters  $g_c$  and  $\Omega_c$ . According to Eq. (10a), the photon-number fluctuation of the coherent field can cause reduction of the Kerr nonlinearity. This effect is remarkable when  $N_c$  is small, as shown in Fig. 2. When  $N_c$  increases to a large number, the contribution of the relative fluctuation  $\Delta N_c^2 / N_c^2$  becomes small and the nonlinear coefficient  $\eta_{\text{CFC}}$  rapidly approaches that of the VIC configuration. In stark contrast, the Kerr photonic nonlinearity in the VIC configuration  $\eta_{\text{VIC}}$  is free of the fluctuation of the coherent control field. Then we call this nonlinearity the shot-noise-suppressing Kerr nonlinearity, meaning it excludes the noise from the photon-number fluctuation of a control field. This property suppressing the control-field noise reveals great advantages in quantum information technologies relying on the Kerr nonlinearity, such as photon blockade.

#### IV. ADVANTAGES IN PHOTON BLOCKADE

The strength of available Kerr nonlinearity in a quantum optical system directly determines the performance of photon

blockade, which is usually used to extract a single photon from a weak coherent probe field [26]. According to the input-output relation [46], we have  $\hat{a}_{\text{out}} = \sqrt{2\kappa_{p,e2}} \hat{a}$  in both configurations. The statistical properties of the output photon mode is the same as that in the probe cavity. Its average is evaluated with the steady-state second-order correlation function at zero delay:

$$g^{(2)}(0) = \frac{\langle \hat{a}_{\text{out}}^\dagger(t) \hat{a}_{\text{out}}^\dagger(t) \hat{a}_{\text{out}}(t) \hat{a}_{\text{out}}(t) \rangle_{\text{SS}}}{\langle \hat{a}_{\text{out}}^\dagger(t) \hat{a}_{\text{out}}(t) \rangle_{\text{SS}}^2}. \quad (11)$$

It is difficult to solve the exact analytical solution of the second-order correlation function. In a weak-driving regime ( $\alpha_{\text{in}} \ll \kappa_p$ ), we truncate the Hilbert space to  $n = 2$  for analytically solving the Schrödinger equation of the system. We obtain the approximate function [47] (see Appendix B)

$$g^{(2)}(0) \approx \frac{\kappa_p^2}{\eta_{\text{VIC}}^2 + \kappa_p^2} \quad (12)$$

at resonance  $\Delta_p = 0$  for the VIC configuration. The Kerr nonlinearity is shot-noise suppressing so that the photon-number fluctuation-induced noise is excluded in  $g^{(2)}(0)$ . However, in the CFC configuration, by substituting Eq. (10a) into Eq. (12) we have

$$g^{(2)}(0) \approx \frac{\kappa_p^2}{\bar{\eta}_{\text{CFC}}^2 + \kappa_p^2} \left( 1 + \frac{\Delta N_c^2}{N_c^2} \right)^2. \quad (13)$$

It can be seen that the fluctuation  $\Delta N_c$  of the coherent control field causes  $g^{(2)}(0)$  to increase and thus weaken the photon blockade effect.

To further evaluate the effect of the coherent control field on the static properties of the outgoing photon mode, we consider the second-order intensity-correlation operator for the output field [3,41]

$$\hat{G} = \hat{a}_{\text{out}}^\dagger \hat{a}_{\text{out}}^\dagger \hat{a}_{\text{out}} \hat{a}_{\text{out}}. \quad (14)$$

In experiments, the field outgoing from the system is split into two paths and measured at the same time or zero delay to obtain the single-shot intensity correlation. Each measurement generates a value of the intensity correlation distributed randomly around its mean value due to the shot noise. The average of a great number of measurement yields the value  $\langle \hat{G} \rangle$ . Normalization by the squared mean intensity of the output field gives the function  $g^{(2)}(0)$ .

Note that the fluctuation of  $\hat{G}$  gives rise to the uncertainty of  $g^{(2)}(0)$  in measurement. In the VIC configuration,  $\hat{G}$  has no contribution from the photon-number fluctuation of the control field but is affected by the probe-field fluctuation. In this sense, the  $g^{(2)}(0)$  is shot-noise suppressing. In the CFC configuration, except for the probe field contribution, the coherent control field also causes extra shot noise to the measurement of  $\hat{G}$ , leading to an additional quantum uncertainty to  $g^{(2)}(0)$ .

The fluctuation of  $\hat{G}$  can be derived approximately as (see Appendix B)

$$\Delta G \approx \frac{8\sqrt{2}\kappa_{p,e1}\kappa_{p,e2}^2\alpha_{\text{in}}^2}{\eta_{\text{VIC}}\kappa_p} \quad (15)$$



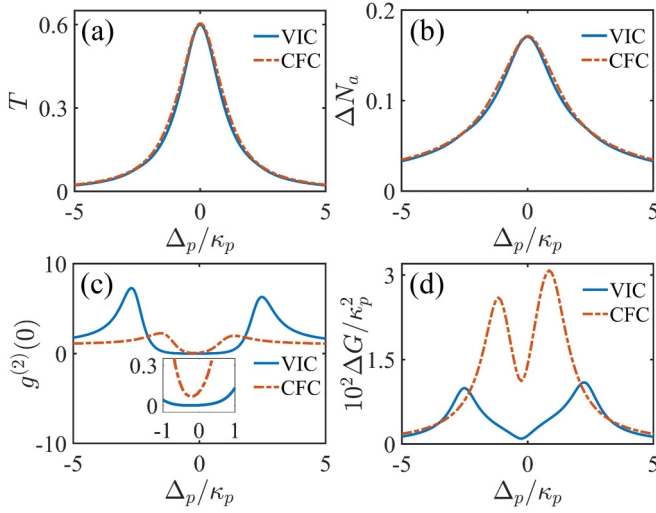


FIG. 3. (a) Transmission and (b) fluctuation  $\Delta N_a$  as a function of the probe-field detuning. (c) Second-order function  $g^{(2)}(0)$  and (d) fluctuation  $\Delta G$  versus the probe-field detuning. The blue and red curves represent the VIC and CFC configurations, respectively. We take  $\kappa_c = \kappa_p$ ,  $g'_c = 67.5\kappa_p$ , and  $\xi = 2\kappa_p$ , yielding  $N_c = 4$  and  $\Omega_c = 135\kappa_p$ . The decay from  $|2\rangle$  to  $|3\rangle$  is  $\gamma_{23} = 0$  and  $\gamma_{23} = 0.1\kappa_p$  in the VIC and CFC configurations, respectively. The other parameters are  $\kappa_{p,i} = 0.2$ ,  $\kappa_{p,e1} = \kappa_{p,e2} = 0.4$ ,  $\kappa_p = 1$ ,  $\gamma_{21} = \gamma_{43} = 0.1\kappa_p$ ,  $\gamma_{42} = \gamma_{31} = 0.001\kappa_p$ ,  $\Delta_{21} = \Delta_{23} = \Delta_{43} = 0.5\kappa_p$ ,  $g_p = 15\kappa_p$ ,  $\alpha_{in}^2 = 0.04\kappa_p$ ,  $g_c = 60\kappa_p$ , and  $\Omega_c = 135\kappa_p$ .

for the VIC configuration and

$$\Delta G \approx \frac{8\sqrt{2}\kappa_{p,e1}\kappa_{p,e2}^2\alpha_{in}^2}{\bar{\eta}_{CFC}\kappa_p} + \frac{8\sqrt{2}\kappa_{p,e1}\kappa_{p,e2}^2\alpha_{in}^2}{\bar{\eta}_{CFC}\kappa_p} \left(\frac{\Delta N_c}{N_c}\right)^2 \quad (16)$$

for the CFC configuration. The first term of Eq. (16) is derived from the photon-number fluctuation of the probe field itself, which we denote by  $\Delta G_p$ . The second term originates from the coherent control field, denoted by  $\Delta G_c$ . Therefore, the use of a coherent control field introduces an additional fluctuation to the second-order correlation function. We go next to the discussion of the transmission of the system, defined as  $T = \langle \hat{a}_{out}^\dagger \hat{a}_{out} \rangle / |\alpha_{in}|^2$ . It is proportional to  $\langle \hat{a}^\dagger \hat{a} \rangle$ . Therefore, its fluctuation is only dependent on the photon-number fluctuation of the probe field given by (see Appendix B)

$$\Delta N_a \approx \sqrt{2\kappa_{p,e1}\alpha_{in}^2 / [(\Delta_p + \delta\omega_x)^2 + \kappa_p^2]}, \quad (17)$$

with  $x = \text{VIC, CFC}$ . Note that  $\Delta N_a$  is unaffected by the photon-number fluctuation of the control field. Hence, the transmissions and their fluctuation in both the VIC and CFC configurations are almost identical [see Figs. 3(a) and 3(b)].

To confirm our analytical results, now we numerically study the full quantum dynamics of both the VIC and CFC configurations by solving the quantum master equation (4) based on Eqs. (1) and (3) with the same parameters for comparison. Figures 3(a) and 3(b) show the same transmissions and corresponding fluctuations for both cases as a function of  $\Delta_p$ . The statistical properties of the output photons, however, are quite different. As expected from the analysis above, the fluctuation  $\Delta N_c$  weakens the photon blockade effect and gives rise to a larger  $g^{(2)}(0)$  in the CFC

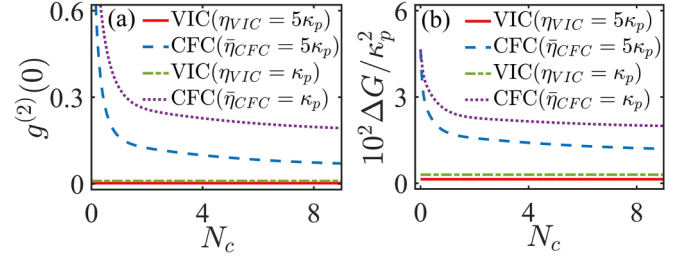


FIG. 4. (a) Second-order function  $g^{(2)}(0)$  and (b) fluctuation  $\Delta G$  versus the quantum-averaged photon number  $N_c$  of the coherent control field. Red solid (blue dashed) solid curves indicate the case of a strong nonlinearity  $\eta_{VIC} = 5\kappa_p$  ( $\bar{\eta}_{CFC} = 5\kappa_p$ ) in the VIC (CFC) configuration with the parameters  $g_p = 15\kappa_p$ ,  $\gamma_{23} = 0$ , and  $g_c = 60\kappa_p$  ( $g_p = 15\kappa_p$ ,  $\gamma_{23} = 0.1\kappa_p$ , and  $\Omega_c = 135\kappa_p$ ). Green dash-dotted (purple dotted) curves represent the case of a weak nonlinearity  $\eta_{VIC} = \kappa_p$  ( $\bar{\eta}_{CFC} = \kappa_p$ ) in the VIC (CFC) configuration with the parameters  $g_p = 10\kappa_p$ ,  $\gamma_{23} = 0$ , and  $g_c = 40\kappa_p$  ( $g_p = 10\kappa_p$ ,  $\gamma_{23} = 0.1\kappa_p$ , and  $\Omega_c = 90\kappa_p$ ). The other parameters are  $\kappa_{p,i} = 0.2$ ,  $\kappa_{p,e1} = \kappa_{p,e2} = 0.4$ ,  $\kappa_p = 1$ ,  $\gamma_{21} = \gamma_{43} = 0.1\kappa_p$ ,  $\gamma_{42} = \gamma_{31} = 0.001\kappa_p$ ,  $\Delta_p = 0$ ,  $\Delta_{21} = \Delta_{23} = \Delta_{43} = 0.5\kappa_p$ , and  $\alpha_{in}^2 = 0.04\kappa_p$ .

configuration [see Fig. 3(c)]. At  $\Delta_p = 0$ , the second-order correlation function  $g^{(2)}(0)$  is 0.003 and 0.1 in the VIC and CFC configurations, respectively. As shown in Fig. 3(d), the fluctuation of the second-order intensity correlation  $\Delta G$  in the VIC configuration is considerably smaller than that in the CFC configuration, because the additional quantum fluctuation  $\Delta N_c$  in the latter case adds an extra contribution to  $\Delta G_c$ . This smaller  $\Delta G$  implies an important advantage of the VIC protocol in photon blockade. Figure 4 shows  $g^{(2)}(0)$  and  $\Delta G$  versus  $N_c$ . When  $N_c$  varies, we keep  $g_c$  and  $\Omega_c$  unchanged, resulting in the same Kerr-type photonic nonlinearity  $\eta_{VIC} = \bar{\eta}_{CFC}$ . In the VIC configuration,  $g^{(2)}(0)$  and  $\Delta G$  are constant since they are independent of  $N_c$ . The performance of photon blockade is thus stable in the VIC protocol. In stark contrast, due to the fluctuation  $\Delta N_c$ ,  $g^{(2)}(0)$  and  $\Delta G$  are strongly dependent on  $N_c$  in the CFC configuration. It can be seen from Fig. 4 that  $g^{(2)}(0)$  and  $\Delta G$  have large values when  $N_c$  is small. With the increase of  $N_c$ , they decrease and eventually converge with that of the VIC configuration. It is worth noting that the weaker the nonlinearity is, the slower  $g^{(2)}(0)$  and  $\Delta G$  decrease with  $N_c$ , and the higher stable value  $g^{(2)}(0)$  and  $\Delta G$  approach (see the blue dashed curve for a strong nonlinearity  $\eta_{VIC} = \bar{\eta}_{CFC} = 5\kappa_p$  and the purple dotted curve for a weak nonlinearity  $\eta_{VIC} = \bar{\eta}_{CFC} = \kappa_p$ ). This implies that, under a weak nonlinear condition, the VIC protocol shows a larger advantage than the CFC protocol in photon blockade for a small  $N_c$ . Due to the limitation of available computation resources, we perform simulations to a small  $N_c$ . In practice, to approach the comparable performance as the VIC protocol, the coherent control field needs to be very strong, corresponding to a large  $N_c$ , which goes beyond the computation capability of a classical computer.

## V. CONCLUSION

We have shown an essential advantage of the VIC protocol over the CFC protocol in quantum manipulation. A shot-noise-suppressing quantum nonlinearity is created by virtue

of the VIC in a cavity QED. As a result, a more stable and stronger photon blockade effect is obtained, in comparison with the conventional CFC-based method. Our VIC-based method using the quantum vacuum field will greatly enrich quantum information technologies. With the help of the VIC, one can construct a three- or four-level superconducting quantum system [32,34], thus boosting quantum information technologies based on nonlinear quantum optics. Moreover, the proposed VIC protocol for quantum manipulation provides a good platform for investigating the nature of the quantum vacuum field.

### ACKNOWLEDGMENTS

This work was supported by the National Key R&D Program of China (Grants No. 2019YFA0308700, No. 2019YFA0308704, and No. 2017YFA0303703), the National Natural Science Foundation of China (Grants No. 11874212 and No. 11890704), the Program for Innovative Talents and Teams in Jiangsu (Grant No. JSSCTD202138), and the Excellent Research Program of Nanjing University (Grant No. ZYJH002).

### APPENDIX A: EFFECTIVE QUANTUM NONLINEARITY COEFFICIENTS OF THE VIC AND CFC CONFIGURATIONS

Using the perturbation approach [2,31,32,43–45], we can obtain the effective quantum nonlinear coefficients of the VIC and CFC configurations. We first derive the VIC configuration. The system consists of a two-level QE, an auxiliary cavity, and a probe cavity. The operators  $\hat{\sigma}^+ = |e\rangle\langle g|$  and  $\hat{\sigma}^- = |g\rangle\langle e|$  stand for the energy transition of the two-level QE. The probe cavity mode  $\hat{a}$  (the auxiliary cavity mode  $\hat{d}$ ) couples to the two-level QE with a strength  $g_p$  ( $g_c$ ). The auxiliary cavity is in the vacuum state and without any external drive. In the case of a weak probe and  $g_p \ll g_c$ , we can truncate the cavity mode  $\hat{d}$  up to the first excited Fock state  $|1_d\rangle$  and thus obtain the state space of a subsystem consisting of the two-level QE and the auxiliary cavity [32]  $|1\rangle_V = |g, 0_d\rangle$ ,  $|2\rangle_V = |e, 0_d\rangle$ ,  $|3\rangle_V = |g, 1_d\rangle$ , and  $|4\rangle_V = |e, 1_d\rangle$ , respectively. This subsystem can be modeled as an  $N$ -type four-level system. We define  $\hat{s}_{mn} = |m\rangle\langle n|_V$  ( $n, m = 1, 2, 3, 4$ ) to describe the transition of the  $N$ -type four-level structure. Therefore, in the basis of  $\{|1\rangle_V, |2\rangle_V, |3\rangle_V, |4\rangle_V\}$ , the Hamiltonian of the VIC configuration is given by

$$\hat{H}_{\text{VIC}} = \hat{H}_{\text{VIC}}^S + \hat{H}_{\text{VIC}}^P, \quad (\text{A1a})$$

$$\begin{aligned} \hat{H}_{\text{VIC}}^S &= \Delta_{21}\hat{s}_{22} + (\Delta_{21} - \Delta_{23})\hat{s}_{33} + (\Delta_{43} + \Delta_{21} - \Delta_{23})\hat{s}_{44} \\ &+ [g_p(\hat{a}^\dagger\hat{s}_{12} + \hat{a}^\dagger\hat{s}_{34}) + g_p(\hat{s}_{21}\hat{a} + \hat{s}_{43}\hat{a})] \\ &+ g_c(\hat{s}_{23} + \hat{s}_{32}), \end{aligned} \quad (\text{A1b})$$

$$\hat{H}_{\text{VIC}}^P = i\sqrt{2\kappa_{p,e1}}\alpha_{\text{in}}(\hat{a}^\dagger e^{-i\Delta_p t} - \hat{a}e^{i\Delta_p t}). \quad (\text{A1c})$$

The decay of the system can be described by the Lindblad operator

$$\begin{aligned} \mathcal{L}\hat{O} &= \kappa_p(2\hat{a}^\dagger\hat{O}\hat{a} - \hat{a}^\dagger\hat{a}\hat{O} - \hat{O}\hat{a}^\dagger\hat{a}) \\ &+ \kappa_d(2\hat{d}^\dagger\hat{O}\hat{d} - \hat{d}^\dagger\hat{d}\hat{O} - \hat{O}\hat{d}^\dagger\hat{d}) \\ &+ \frac{\gamma}{2}(2\hat{\sigma}^+\hat{O}\hat{\sigma}^- - \hat{\sigma}^+\hat{\sigma}^-\hat{O} - \hat{O}\hat{\sigma}^+\hat{\sigma}^-). \end{aligned} \quad (\text{A2})$$

Here  $\kappa_p = \kappa_{p,e1} + \kappa_{p,i} + \kappa_{p,e2}$  is from the total decay of the probe cavity,  $\kappa_d = \kappa_{d,i}$  accounts for the loss of the auxiliary cavity, and the relaxation rate  $\gamma$  results from the two-level QE. Expanding operators  $\hat{d}^\dagger$  and  $\hat{\sigma}^+$  under the basis  $\{|1\rangle_V, |2\rangle_V, |3\rangle_V, |4\rangle_V\}$ , we have

$$\begin{aligned} \hat{d}^\dagger &= (|e\rangle\langle e| + |g\rangle\langle g|) \otimes |1_d\rangle\langle 0_d| = \hat{s}_{42} + \hat{s}_{31}, \\ \hat{\sigma}^+ &= |e\rangle\langle g| \otimes (|1_d\rangle\langle 1_d| + |0_d\rangle\langle 0_d|) = \hat{s}_{21} + \hat{s}_{43}. \end{aligned} \quad (\text{A3})$$

Then substituting Eq. (A3) into Eq. (A2) and neglecting cross terms, we get

$$\begin{aligned} \mathcal{L}\hat{O} &= \kappa_p(2\hat{a}^\dagger\hat{O}\hat{a} - \hat{a}^\dagger\hat{a}\hat{O} - \hat{O}\hat{a}^\dagger\hat{a}) \\ &+ \kappa_d(2\hat{s}_{42}\hat{O}\hat{s}_{24} - \hat{s}_{44}\hat{O} - \hat{O}\hat{s}_{44}) \\ &+ \kappa_d(2\hat{s}_{31}\hat{O}\hat{s}_{31} - \hat{s}_{33}\hat{O} - \hat{O}\hat{s}_{33}) \\ &+ \frac{\gamma}{2}(2\hat{s}_{21}\hat{O}\hat{s}_{12} - \hat{s}_{22}\hat{O} - \hat{O}\hat{s}_{22}) \\ &+ \frac{\gamma}{2}(2\hat{s}_{43}\hat{O}\hat{s}_{34} - \hat{s}_{44}\hat{O} - \hat{O}\hat{s}_{44}), \end{aligned} \quad (\text{A4})$$

where the second (third) term describes the decay from  $|4\rangle_V$  ( $|3\rangle_V$ ) to  $|2\rangle_V$  ( $|1\rangle_V$ ) by the loss of the auxiliary cavity mode and the fourth (last) term describes the decay from  $|2\rangle_V$  ( $|4\rangle_V$ ) to  $|1\rangle_V$  ( $|3\rangle_V$ ) by the relaxation of the two-level QE. We take  $\gamma_{42} = \gamma_{31} = 2\kappa_d = 2\kappa_{d,i}$  and  $\gamma_{21} = \gamma_{43} = \gamma$ . It is worth noting that the state  $|2\rangle_V$  does not decay to the state  $|3\rangle_V$ , that is,  $\gamma_{23} = 0$ . This is because the coherent process between  $|2\rangle_V$  and  $|3\rangle_V$  is induced by QE-cavity coupling, which is different from the typical decoherence mechanism in the conventional  $N$ -type four-level structure. Therefore, the Lindblad operator can be rewritten as

$$\mathcal{L}[\Gamma, \hat{A}]\hat{O} = \Gamma(2\hat{A}^\dagger\hat{O}\hat{A} - \hat{A}^\dagger\hat{A}\hat{O} - \hat{O}\hat{A}^\dagger\hat{A}), \quad (\text{A5})$$

where  $\Gamma = \{\kappa_p, \gamma_{21}/2, \gamma_{23}/2, \gamma_{31}/2, \gamma_{43}/2, \gamma_{42}/2\}$  represents the decay rate of each state analyzed in the main text and  $\hat{A} = \{\hat{a}, \hat{s}_{12}, \hat{s}_{32}, \hat{s}_{13}, \hat{s}_{34}, \hat{s}_{24}\}$ . Then the Heisenberg equations for the system in the VIC configuration take the form ( $\gamma_{23} = 0$ )

$$\dot{\hat{a}} = -\kappa_p\hat{a} - ig_p\hat{s}_{12} - ig_p\hat{s}_{34} + \sqrt{2\kappa_{p,e1}}\alpha_{\text{in}}e^{-i\Delta_p t}, \quad (\text{A6a})$$

$$\dot{\hat{s}}_{11} = \gamma_{21}\hat{s}_{22} + \gamma_{31}\hat{s}_{33} - ig_p(\hat{a}^\dagger\hat{s}_{12} - \hat{s}_{21}\hat{a}), \quad (\text{A6b})$$

$$\begin{aligned} \dot{\hat{s}}_{22} &= -(\gamma_{21} + \gamma_{23})\hat{s}_{22} + \gamma_{42}\hat{s}_{44} + ig_p(\hat{a}^\dagger\hat{s}_{12} - \hat{s}_{21}\hat{a}) \\ &- ig_c(\hat{s}_{23} - \hat{s}_{32}), \end{aligned} \quad (\text{A6c})$$

$$\begin{aligned} \dot{\hat{s}}_{33} &= -\gamma_{31}\hat{s}_{33} + \gamma_{23}\hat{s}_{22} + \gamma_{43}\hat{s}_{44} - ig_p(\hat{a}^\dagger\hat{s}_{34} - \hat{s}_{43}\hat{a}) \\ &+ ig_c(\hat{s}_{23} - \hat{s}_{32}), \end{aligned} \quad (\text{A6d})$$

$$\dot{\hat{s}}_{44} = -(\gamma_{42} + \gamma_{43})\hat{s}_{44} + ig_p(\hat{a}^\dagger\hat{s}_{34} - \hat{s}_{43}\hat{a}), \quad (\text{A6e})$$

$$\dot{\hat{s}}_{23} = -\tilde{\gamma}_{23}\hat{s}_{23} + ig_c(\hat{s}_{33} - \hat{s}_{22}) + ig_p\hat{a}^\dagger(\hat{s}_{13} - \hat{s}_{24}), \quad (\text{A6f})$$

$$\dot{\hat{s}}_{14} = -\tilde{\gamma}_{41}\hat{s}_{14} + ig_p(\hat{s}_{24} - \hat{s}_{13})\hat{a}, \quad (\text{A6g})$$

$$\dot{\hat{s}}_{12} = -\tilde{\gamma}_{21}\hat{s}_{12} - ig_c\hat{s}_{13} - ig_p(\hat{s}_{11} - \hat{s}_{22})\hat{a}, \quad (\text{A6h})$$

$$\dot{\hat{s}}_{13} = -\tilde{\gamma}_{31}\hat{s}_{13} - ig_c\hat{s}_{12} + ig_p(\hat{s}_{23}\hat{a} - \hat{a}^\dagger\hat{s}_{14}), \quad (\text{A6i})$$

$$\dot{\hat{s}}_{24} = -\tilde{\gamma}_{24}\hat{s}_{24} + ig_c\hat{s}_{34} + ig_p(\hat{a}^\dagger\hat{s}_{14} - \hat{s}_{23}\hat{a}), \quad (\text{A6j})$$

$$\dot{\hat{s}}_{34} = -\tilde{\gamma}_{34}\hat{s}_{34} + ig_c\hat{s}_{24} - ig_p(\hat{s}_{33} - \hat{s}_{44})\hat{a}, \quad (\text{A6k})$$

where  $\tilde{\gamma}_2 = (\gamma_{21} + \gamma_{23})/2 + i\Delta_{21}$ ,  $\tilde{\gamma}_3 = \gamma_{31}/2 + i(\Delta_{21} - \Delta_{23})$ ,  $\tilde{\gamma}_4 = (\gamma_{42} + \gamma_{43})/2 + i(\Delta_{43} + \Delta_{21} - \Delta_{23})$ ,  $\tilde{\gamma}_{23} = (\gamma_{21} + \gamma_{23} + \gamma_{31})/2 - i\Delta_{23}$ ,  $\tilde{\gamma}_{24} = (\gamma_{21} + \gamma_{23} + \gamma_{42} +$

$\gamma_{43})/2 + i(\Delta_{43} - \Delta_{23})$ , and  $\tilde{\gamma}_{34} = (\gamma_{31} + \gamma_{42} + \gamma_{43})/2 + i\Delta_{43}$ .

The transition operator can be expanded as  $\hat{s}_{mn} = \hat{s}_{mn}^{(0)} + \hat{s}_{mn}^{(1)} + \hat{s}_{mn}^{(2)} + \hat{s}_{mn}^{(3)} + \dots$ . In the case of a weak probe and  $g_p \ll g_c$ , the system is mostly populated in the ground state  $|1\rangle_V$ . Hence, to a good approximation, all the populations can be assumed in the ground state  $|1\rangle_V$  to zeroth order, i.e.,  $\hat{s}_{11}^{(0)} = 1$ ,  $\hat{s}_{22}^{(0)} = \hat{s}_{33}^{(0)} = \hat{s}_{44}^{(0)} = 0$ . The terms with  $\hat{s}_{mn}g_p$  ( $m \neq n$ ) can be neglected when solving  $\hat{s}_{mn}$ . Then we have the first-order solutions for the operators

$$\hat{s}_{12}^{(1)} = -\frac{ig_p}{g_c^2 F} \hat{a}, \quad (\text{A7a})$$

$$\hat{s}_{13}^{(1)} = -\frac{ig_c}{\tilde{\gamma}_3 + g_p^2 N_a / \tilde{\gamma}_4} \hat{s}_{12}^{(1)}, \quad (\text{A7b})$$

with  $F = \tilde{\gamma}_2/g_c^2 + 1/(\tilde{\gamma}_3 + g_p^2 N_a / \tilde{\gamma}_4)$ , where  $N_a$  is the average photon number of the probe field. As for a closed system, the total population is conserved, i.e.,  $\hat{s}_{11} + \hat{s}_{22} + \hat{s}_{33} + \hat{s}_{44} = 1$ . The second-order population operators satisfy the relationship

$$\hat{s}_{11}^{(2)} + \hat{s}_{22}^{(2)} + \hat{s}_{33}^{(2)} + \hat{s}_{44}^{(2)} = 0. \quad (\text{A8})$$

Substituting Eqs. (A7) and (A8) into Eqs. (A6b)–(A6e), we obtain the second-order population operators

$$\hat{s}_{11}^{(2)} = -\frac{(\gamma_{23} + \gamma_{31})g_p^2}{\gamma_{31}(\gamma_{21} + \gamma_{23})g_c^2} \left( \frac{1}{F} + \frac{1}{F^*} \right) \hat{a}^\dagger \hat{a}, \quad (\text{A9a})$$

$$\hat{s}_{22}^{(2)} = \frac{g_p^2}{(\gamma_{21} + \gamma_{23})g_c^2} \left( \frac{1}{F} + \frac{1}{F^*} \right) \hat{a}^\dagger \hat{a}. \quad (\text{A9b})$$

Similarly, substituting Eqs. (A9) into Eqs. (A6f)–(A6k), we get the operators  $\hat{s}_{12}^{(3)}$  and  $\hat{s}_{34}^{(3)}$  to third order,

$$\hat{s}_{12}^{(3)} = \frac{ig_p^3(2\gamma_{31} + \gamma_{23})}{g_c^4 \gamma_{31}(\gamma_{21} + \gamma_{23})F} \left( \frac{1}{F} + \frac{1}{F^*} \right) \hat{a}^\dagger \hat{a} \hat{a}, \quad (\text{A10a})$$

$$\hat{s}_{34}^{(3)} = 0. \quad (\text{A10b})$$

Therefore, we have

$$\hat{s}_{12} = \hat{s}_{12}^{(1)} + \hat{s}_{12}^{(3)}, \quad (\text{A11a})$$

$$\hat{s}_{34} = 0. \quad (\text{A11b})$$

For an observable  $\hat{O}$ , related to the cavity mode  $\hat{a}$ , we can obtain the relation from the quantum master equation

$$\begin{aligned} \dot{\hat{O}} = & -ig_p([\hat{O}, \hat{a}^\dagger]\hat{s}_{12} + \hat{s}_{21}[\hat{O}, \hat{a}]) \\ & -ig_p([\hat{O}, \hat{a}^\dagger]\hat{s}_{34} + \hat{s}_{43}[\hat{O}, \hat{a}]) \\ & + \kappa_p(2\hat{a}^\dagger \hat{O} \hat{a} - \hat{a}^\dagger \hat{a} \hat{O} - \hat{O} \hat{a}^\dagger \hat{a}) \\ & + \sqrt{2\kappa_{p,e1}}\alpha_{\text{in}}[\hat{O}, \hat{a}^\dagger e^{-i\Delta_p t} - \hat{a} e^{i\Delta_p t}]. \end{aligned} \quad (\text{A12})$$

Thus, substituting Eqs. (A11) into Eq. (A12), we have

$$\begin{aligned} \dot{\hat{O}} = & -i\delta\omega_{\text{VIC}}[\hat{O}, \hat{a}^\dagger \hat{a}] - i\eta_{\text{VIC}}[\hat{O}, \hat{a}^\dagger \hat{a}^\dagger \hat{a} \hat{a}] \\ & + \kappa_{\text{VIC}}^L(2\hat{a}^\dagger \hat{O} \hat{a} - \hat{a}^\dagger \hat{a} \hat{O} - \hat{O} \hat{a}^\dagger \hat{a}) \\ & + \kappa_{\text{VIC}}^{NL}(2\hat{a}^{\dagger 2} \hat{O} \hat{a}^2 - \hat{a}^{\dagger 2} \hat{a}^2 \hat{O} - \hat{O} \hat{a}^{\dagger 2} \hat{a}^2) \\ & + \kappa_p(2\hat{a}^\dagger \hat{O} \hat{a} - \hat{a}^\dagger \hat{a} \hat{O} - \hat{O} \hat{a}^\dagger \hat{a}) \\ & + \sqrt{2\kappa_{p,e1}}\alpha_{\text{in}}[\hat{O}, \hat{a}^\dagger e^{-i\Delta_p t} - \hat{a} e^{i\Delta_p t}], \end{aligned} \quad (\text{A13})$$

where

$$\delta\omega_{\text{VIC}} = -\frac{\text{Im}(F)g_p^2}{g_c^2|F|^2}, \quad (\text{A14a})$$

$$\eta_{\text{VIC}} = \frac{g_p^4(2\gamma_{31} + \gamma_{23})}{g_c^4 \gamma_{31}(\gamma_{21} + \gamma_{23})} \left( \frac{1}{F} + \frac{1}{F^*} \right) \frac{\text{Im}(F)}{|F|^2}, \quad (\text{A14b})$$

$$\kappa_{\text{VIC}}^L = \frac{\text{Re}(F)g_p^2}{g_c^2|F|^2}, \quad (\text{A14c})$$

$$\kappa_{\text{VIC}}^{NL} = -\frac{g_p^4(2\gamma_{31} + \gamma_{23})}{g_c^4 \gamma_{31}(\gamma_{21} + \gamma_{23})} \left( \frac{1}{F} + \frac{1}{F^*} \right) \frac{\text{Re}(F)}{|F|^2}. \quad (\text{A14d})$$

From Eq. (A13) we can see that  $\delta\omega_{\text{VIC}}$  and  $\eta_{\text{VIC}}$  describe the linear frequency shift and the quantum nonlinearity of the VIC configuration, respectively. Here  $\kappa_{\text{VIC}}^L$  and  $\kappa_{\text{VIC}}^{NL}$  are the linear decay rate and the nonlinear dissipation, respectively. Under the condition of two-photon resonance  $\Delta_{21} = \Delta_{23}$ , the linear frequency shift  $\delta\omega_{\text{VIC}} \approx 0$  and the linear decay rate  $\kappa_{\text{VIC}}^L \approx 0$  [37]. In the case of  $|\Delta_{43}| > 0$ , the nonlinear dissipation  $|\kappa_{\text{VIC}}^{NL}| \ll |\eta_{\text{VIC}}|$ ; thus it can be neglected in our paper [37,44]. It is worth noting that when we take  $\Delta_{43} = 0$ , the dispersion of the system is negligible, meaning  $\eta_{\text{VIC}} \approx 0$ , while the nonlinear dissipation is large. This mechanism enables nonlinear dissipation-induced photon blockade [48].

Now we consider the CFC configuration. The Hamiltonian of the pseudocavity QED system reads

$$\hat{H}_{\text{CFC}} = \hat{H}_{\text{CFC}}^S + \hat{H}_{\text{CFC}}^P, \quad (\text{A15a})$$

$$\begin{aligned} \hat{H}_{\text{CFC}}^S = & \Delta_{21}\hat{\sigma}_{22} + (\Delta_{21} - \Delta_{23})\hat{\sigma}_{33} + (\Delta_{43} + \Delta_{21} - \Delta_{23})\hat{\sigma}_{44} \\ & + [g_p(\hat{a}^\dagger \hat{\sigma}_{12} + \hat{a}^\dagger \hat{\sigma}_{34}) + g'_c \hat{c}^\dagger \hat{\sigma}_{32} + \text{H.c.}] \\ & + i\xi(\hat{c}^\dagger - \hat{c}), \end{aligned} \quad (\text{A15b})$$

$$\hat{H}_{\text{CFC}}^P = i\sqrt{2\kappa_{p,e1}}\alpha_{\text{in}}(\hat{a}^\dagger e^{-i\Delta_p t} - \hat{a} e^{i\Delta_p t}). \quad (\text{A15c})$$

The Lindblad operator is given by

$$\mathcal{L}[\Gamma, \hat{A}]\hat{O} = \Gamma(2\hat{A}^\dagger \hat{O} \hat{A} - \hat{A}^\dagger \hat{A} \hat{O} - \hat{O} \hat{A}^\dagger \hat{A}), \quad (\text{A16})$$

where  $\Gamma = \{\kappa_p, \kappa_c, \gamma_{21}/2, \gamma_{23}/2, \gamma_{31}/2, \gamma_{43}/2, \gamma_{42}/2\}$  represents the decay rate of each state and  $\hat{A} = \{\hat{a}, \hat{c}, \hat{\sigma}_{12}, \hat{\sigma}_{32}, \hat{\sigma}_{13}, \hat{\sigma}_{34}, \hat{\sigma}_{24}\}$ . The decay rate  $\kappa_c$  results from the pseudocavity mode  $\hat{c}$ . The Heisenberg equations for the pseudocavity QED system take the form

$$\dot{\hat{a}} = -\kappa_p \hat{a} - ig_p \hat{\sigma}_{12} - ig_p \hat{\sigma}_{34} + \sqrt{2\kappa_{p,e1}}\alpha_{\text{in}} e^{-i\Delta_p t}, \quad (\text{A17a})$$

$$\dot{\hat{\sigma}}_{11} = \gamma_{21} \hat{\sigma}_{22} + \gamma_{31} \hat{\sigma}_{33} - ig_p(\hat{a}^\dagger \hat{\sigma}_{12} - \hat{\sigma}_{21} \hat{a}), \quad (\text{A17b})$$

$$\begin{aligned} \dot{\hat{\sigma}}_{22} = & -(\gamma_{21} + \gamma_{23})\hat{\sigma}_{22} + \gamma_{42}\hat{\sigma}_{44} + ig_p(\hat{a}^\dagger \hat{\sigma}_{12} - \hat{\sigma}_{21} \hat{a}) \\ & - ig'_c(\hat{\sigma}_{23} \hat{c} - \hat{c}^\dagger \hat{\sigma}_{32}), \end{aligned} \quad (\text{A17c})$$

$$\begin{aligned} \dot{\hat{\sigma}}_{33} = & -\gamma_{31}\hat{\sigma}_{33} + \gamma_{23}\hat{\sigma}_{22} + \gamma_{43}\hat{\sigma}_{44} - ig_p(\hat{a}^\dagger \hat{\sigma}_{34} - \hat{\sigma}_{43} \hat{a}) \\ & + ig'_c(\hat{\sigma}_{23} \hat{c} - \hat{c}^\dagger \hat{\sigma}_{32}), \end{aligned} \quad (\text{A17d})$$

$$\dot{\hat{\sigma}}_{44} = -(\gamma_{42} + \gamma_{43})\hat{\sigma}_{44} + ig_p(\hat{a}^\dagger \hat{\sigma}_{34} - \hat{\sigma}_{43} \hat{a}), \quad (\text{A17e})$$

$$\begin{aligned} \dot{\hat{\sigma}}_{23} = & -\tilde{\gamma}_{23}\hat{\sigma}_{23} + ig'_c \hat{c}^\dagger (\hat{\sigma}_{33} - \hat{\sigma}_{22}) \\ & + ig_p \hat{a}^\dagger (\hat{\sigma}_{13} - \hat{\sigma}_{24}), \end{aligned} \quad (\text{A17f})$$

$$\dot{\hat{\sigma}}_{14} = -\tilde{\gamma}_4 \hat{\sigma}_{14} + ig_p(\hat{\sigma}_{24} - \hat{\sigma}_{13}) \hat{a}, \quad (\text{A17g})$$

$$\dot{\hat{\sigma}}_{12} = -\tilde{\gamma}_2 \hat{\sigma}_{12} - ig'_c \hat{\sigma}_{13} \hat{c} - ig_p(\hat{\sigma}_{11} - \hat{\sigma}_{22}) \hat{a}, \quad (\text{A17h})$$

$$\dot{\hat{\sigma}}_{13} = -\tilde{\gamma}_3 \hat{\sigma}_{13} - ig'_c \hat{c}^\dagger \hat{\sigma}_{12} + ig_p (\hat{\sigma}_{23} \hat{a} - \hat{a}^\dagger \hat{\sigma}_{14}), \quad (\text{A17i})$$

$$\dot{\hat{\sigma}}_{24} = -\tilde{\gamma}_{24} \hat{\sigma}_{24} + ig'_c \hat{c}^\dagger \hat{\sigma}_{34} + ig_p (\hat{a}^\dagger \hat{\sigma}_{14} - \hat{\sigma}_{23} \hat{a}), \quad (\text{A17j})$$

$$\dot{\hat{\sigma}}_{34} = -\tilde{\gamma}_{34} \hat{\sigma}_{34} + ig'_c \hat{\sigma}_{24} \hat{c} - ig_p (\hat{\sigma}_{33} - \hat{\sigma}_{44}) \hat{a}, \quad (\text{A17k})$$

where  $\tilde{\gamma}_2 = (\gamma_{21} + \gamma_{23})/2 + i\Delta_{21}$ ,  $\tilde{\gamma}_3 = \gamma_{31}/2 + i(\Delta_{21} - \Delta_{23})$ ,  $\tilde{\gamma}_4 = (\gamma_{42} + \gamma_{43})/2 + i(\Delta_{43} + \Delta_{21} - \Delta_{23})$ ,  $\tilde{\gamma}_{23} = (\gamma_{21} + \gamma_{23} + \gamma_{31})/2 - i\Delta_{23}$ ,  $\tilde{\gamma}_{24} = (\gamma_{21} + \gamma_{23} + \gamma_{42} + \gamma_{43})/2 + i(\Delta_{43} - \Delta_{23})$ , and  $\tilde{\gamma}_{34} = (\gamma_{31} + \gamma_{42} + \gamma_{43})/2 + i\Delta_{43}$ .

From Eq. (A17) it can be found that the pseudocavity QED model provides an opportunity to evaluate the influence of photon-number fluctuations of the control field  $\hat{c}$  we are interested in. By performing the same calculation steps to adiabatically eliminate the atomic operators ( $\hat{\sigma}_{nm}$ ) and retain operators of the control field ( $\hat{c}$  and  $\hat{c}^\dagger$ ), we have the first-order solutions

$$\hat{\sigma}_{12}^{(1)} = -\frac{ig_p}{g_c^2 F} \hat{a}, \quad (\text{A18a})$$

$$\hat{\sigma}_{13}^{(1)} = -\frac{ig'_c \hat{c}^\dagger}{\tilde{\gamma}_3 + g_p^2 N_a / \tilde{\gamma}_4} \hat{\sigma}_{12}^{(1)} \quad (\text{A18b})$$

and the third-order solutions

$$\hat{\sigma}_{12}^{(3)} = \frac{ig_p^3 (2\gamma_{31} + \gamma_{23})}{g_c^4 (\hat{c}^\dagger \hat{c})^2 \gamma_{31} (\gamma_{21} + \gamma_{23}) F} \left( \frac{1}{F} + \frac{1}{F^*} \right) \hat{a}^\dagger \hat{a} \hat{a}, \quad (\text{A19a})$$

$$\hat{\sigma}_{34}^{(3)} = 0. \quad (\text{A19b})$$

Finally, we obtain

$$\hat{\sigma}_{12} = \hat{\sigma}_{12}^{(1)} + \hat{\sigma}_{12}^{(3)}, \quad (\text{A20a})$$

$$\hat{\sigma}_{34} = 0. \quad (\text{A20b})$$

Then the quantum the nonlinear coefficient in the CFC configuration is given

$$\hat{\eta}_{\text{CFC}} = \frac{g_p^4 (2\gamma_{31} + \gamma_{23})}{g_c^4 (\hat{c}^\dagger \hat{c})^2 \gamma_{31} (\gamma_{21} + \gamma_{23})} \left( \frac{1}{F} + \frac{1}{F^*} \right) \frac{\text{Im}(F)}{|F|^2}. \quad (\text{A21})$$

From Eq. (A21) we find that the nonlinearity  $\hat{\eta}_{\text{CFC}}$  related to the photon-number operator  $\hat{c}^\dagger \hat{c}$  of the coherent control field is no longer a pure number but an operator.

Applying a unitary transformation of  $\hat{U} = \exp(i\Delta_p \hat{a}^\dagger \hat{a} t)$  to the system, we can get the effective Hamiltonian

$$\begin{aligned} \hat{H}_{\text{VIC}}^{\text{eff}} &= (\Delta_p + \delta\omega_{\text{VIC}}) \hat{a}^\dagger \hat{a} + \eta_{\text{VIC}} \hat{a}^\dagger \hat{a}^\dagger \hat{a} \hat{a} \\ &+ i\sqrt{2\kappa_{p,e1}} \alpha_{\text{in}} (\hat{a}^\dagger - \hat{a}) \end{aligned} \quad (\text{A22})$$

for the VIC configuration and

$$\begin{aligned} \hat{H}_{\text{CFC}}^{\text{eff}} &= (\Delta_p + \delta\omega_{\text{CFC}}) \hat{a}^\dagger \hat{a} + \hat{\eta}_{\text{CFC}} \hat{a}^\dagger \hat{a}^\dagger \hat{a} \hat{a} \\ &+ i\sqrt{2\kappa_{p,e1}} \alpha_{\text{in}} (\hat{a}^\dagger - \hat{a}) \end{aligned} \quad (\text{A23})$$

for the CFC configuration. As discussed in the main text, the quantum-averaged nonlinear coefficient of the CFC

configuration  $\eta_{\text{CFC}} = \langle \hat{\eta}_{\text{CFC}} \rangle$  can be derived as

$$\eta_{\text{CFC}} = \frac{\bar{\eta}_{\text{CFC}}}{1 + \Delta N_c^2 / N_c^2}, \quad (\text{A24a})$$

$$\bar{\eta}_{\text{CFC}} = \frac{g_p^4 (2\gamma_{31} + \gamma_{23})}{\Omega_c^4 \gamma_{31} (\gamma_{21} + \gamma_{23})} \left( \frac{1}{F} + \frac{1}{F^*} \right) \frac{\text{Im}(F)}{|F|^2}. \quad (\text{A24b})$$

## APPENDIX B: SECOND-ORDER CORRELATION FUNCTION AND FLUCTUATION OF THE SECOND-ORDER CORRELATION OPERATOR

In this Appendix we derive the analytical solution of the second-order correlation function and fluctuation in a weak-driving regime [47]. We first consider the VIC configuration. Taking into account the loss of the probe cavity, the effective Hamiltonian (A22) can be expressed in a number state representation as

$$\begin{aligned} \hat{H}_{\text{VIC}}^{\text{eff}} &= \sum_n [(E_n - in\kappa_p |n\rangle\langle n|) \\ &+ i\sqrt{2\kappa_{p,e1}} \alpha_{\text{in}} \sqrt{n+1} (|n+1\rangle\langle n| - |n\rangle\langle n+1|)], \end{aligned} \quad (\text{B1})$$

where  $E_n = (\Delta_p + \delta\omega_{\text{VIC}})n + n(n-1)\eta_{\text{VIC}}$  represents the eigenvalues. We expand the Hamiltonian in the basis states  $\{|0\rangle, |1\rangle, |2\rangle\}$  for a weak-driving case,

$$\begin{aligned} \hat{H}_{\text{VIC}}^{\text{eff}} &= E_0 |0\rangle\langle 0| + (E_1 - i\kappa_p) |1\rangle\langle 1| + (E_2 - 2i\kappa_p) |2\rangle\langle 2| \\ &+ i\sqrt{2\kappa_{p,e1}} \alpha_{\text{in}} (|1\rangle\langle 0| - |0\rangle\langle 1|) \\ &+ i\sqrt{4\kappa_{p,e1}} \alpha_{\text{in}} (|2\rangle\langle 1| - |1\rangle\langle 2|). \end{aligned} \quad (\text{B2})$$

A general state in this subspace can be written as

$$|\psi(t)\rangle = C_0(t)|0\rangle + C_1(t)|1\rangle + C_2(t)|2\rangle, \quad (\text{B3})$$

with  $|C_0|^2 + |C_1|^2 + |C_2|^2 = 1$ . Substituting Eqs. (B2) and (B3) into the Schrödinger equation

$$i|\dot{\psi}(t)\rangle = \hat{H}_{\text{VIC}}^{\text{eff}} |\psi(t)\rangle, \quad (\text{B4})$$

we obtain

$$i|\dot{\psi}(t)\rangle = i[\dot{C}_0(t)|0\rangle + \dot{C}_1(t)|1\rangle + \dot{C}_2(t)|2\rangle], \quad (\text{B5a})$$

$$\hat{H}_{\text{VIC}}^{\text{eff}} |\psi(t)\rangle = \hat{H}_{\text{VIC}}^{\text{eff}} [C_0(t)|0\rangle + C_1(t)|1\rangle + C_2(t)|2\rangle], \quad (\text{B5b})$$

where

$$\hat{H}_{\text{VIC}}^{\text{eff}} C_0(t)|0\rangle = E_0 C_0(t)|0\rangle + i\sqrt{2\kappa_{p,e1}} \alpha_{\text{in}} C_0(t)|1\rangle, \quad (\text{B6a})$$

$$\begin{aligned} \hat{H}_{\text{VIC}}^{\text{eff}} C_1(t)|1\rangle &= (E_1 - i\kappa_p) C_1(t)|1\rangle + i\alpha_{\text{in}} C_1(t) (\sqrt{4\kappa_{p,e1}} |2\rangle \\ &- \sqrt{2\kappa_{p,e1}} |0\rangle), \end{aligned} \quad (\text{B6b})$$

$$\hat{H}_{\text{VIC}}^{\text{eff}} C_2(t)|2\rangle = (E_2 - 2i\kappa_p) C_2(t)|2\rangle - i\sqrt{4\kappa_{p,e1}} \alpha_{\text{in}} C_2(t)|1\rangle. \quad (\text{B6c})$$

By comparison with the coefficients of the same basis states in Eqs. (B5), we obtain

$$\dot{C}_0(t) = -iE_0 C_0(t) - \alpha_{\text{in}} \sqrt{2\kappa_{p,e1}} C_1(t),$$

$$\begin{aligned} \dot{C}_1(t) &= -i(E_1 - i\kappa_p) C_1(t) + \sqrt{2\kappa_{p,e1}} \alpha_{\text{in}} C_0(t) \\ &- \sqrt{4\kappa_{p,e1}} \alpha_{\text{in}} C_2(t), \end{aligned}$$



$$\dot{C}_2(t) = -i(E_2 - 2i\kappa_p)C_2(t) + \sqrt{4\kappa_{p,e1}}\alpha_{in}C_1(t). \quad (\text{B7})$$

As we analyze in the main text, in the case of a weak probe  $\alpha_{in} < \kappa_p$  and  $g_p \ll g_c$ , the ground state, i.e., the vacuum state, is mostly populated. Thus, we can assume that  $C_0 \sim 1$ . Also, we can approximately solve Eq. (B7) using a perturbation method by discarding higher-order terms [47] and have

$$\begin{aligned} \dot{C}_0(t) &= -iE_0C_0(t), \\ \dot{C}_1(t) &= -i(E_1 - i\kappa_p)C_1(t) + \sqrt{2\kappa_{p,e1}}\alpha_{in}C_0(t), \\ \dot{C}_2(t) &= -i(E_2 - 2i\kappa_p)C_2(t) + \sqrt{4\kappa_{p,e1}}\alpha_{in}C_1(t). \end{aligned} \quad (\text{B8})$$

The probe cavity is initially in a vacuum state, i.e.,  $C_0(0) = 1$  and  $C_1(0) = C_2(0) = 0$ . Hence, the solution of zero-photon amplitude can be solved as

$$C_0(t) = e^{-iE_0t}. \quad (\text{B9})$$

The solution of the single-photon amplitude in Eq. (B8) becomes

$$\dot{C}_1(t) = -i(E_1 - i\kappa_p)C_1(t) + \sqrt{2\kappa_{p,e1}}\alpha_{in}e^{-iE_0t}. \quad (\text{B10})$$

By introducing a slowly varying single-photon amplitude

$$\begin{aligned} C_1(t) &= c_1(t)e^{-i(E_1 - i\kappa_p)t}, \\ C_1(0) &= c_1(0) \end{aligned} \quad (\text{B11})$$

to solve Eq. (B10), we obtain

$$\dot{C}_1(t) = \dot{c}_1(t)e^{-i(E_1 - i\kappa_p)t} - i(E_1 - i\kappa_p)c_1(t)e^{-i(E_1 - i\kappa_p)t}. \quad (\text{B12})$$

Substituting Eqs. (B12) and (B11) into Eq. (B10), we have

$$\dot{c}_1(t) = \sqrt{2\kappa_{p,e1}}\alpha_{in}e^{i(E_1 - E_0 - i\kappa_p)t}. \quad (\text{B13})$$

Integrating both sides of Eq. (B13), the solution is

$$\begin{aligned} c_1(t) &= c_1(0) + \sqrt{2\kappa_{p,e1}}\alpha_{in} \frac{1}{i(E_1 - E_0 - i\kappa_p)} \\ &\times [e^{i(E_1 - E_0 - i\kappa_p)t} - 1] \end{aligned} \quad (\text{B14})$$

and Eq. (B11) becomes

$$\begin{aligned} C_1(t) &= c_1(0)e^{-i(E_1 - i\kappa_p)t} + \sqrt{2\kappa_{p,e1}}\alpha_{in} \frac{1}{i(E_1 - E_0 - i\kappa_p)} \\ &\times [e^{-iE_0t} - e^{-i(E_1 - i\kappa_p)t}]. \end{aligned} \quad (\text{B15})$$

According to the initial condition  $C_1(0) = 0 = c_1(0)$ , we can obtain

$$C_1(t) = \frac{\sqrt{2\kappa_{p,e1}}\alpha_{in}}{i(E_1 - E_0 - i\kappa_p)} [e^{-iE_0t} - e^{-i(E_1 - i\kappa_p)t}]. \quad (\text{B16})$$

Now we derive the two-photon amplitude in Eqs. (B8). Substituting Eq. (B16) into Eqs. (B8), we get

$$\begin{aligned} \dot{C}_2(t) &= -i(E_2 - 2i\kappa_p)C_2(t) \\ &+ \frac{\sqrt{8\kappa_{p,e1}}\alpha_{in}^2}{i(E_1 - E_0 - i\kappa_p)} [e^{-iE_0t} - e^{-i(E_1 - i\kappa_p)t}]. \end{aligned} \quad (\text{B17})$$

Similarly, we introduce slowly varying two-photon amplitude

$$\begin{aligned} C_2(t) &= c_2(t)e^{-i(E_2 - 2i\kappa_p)t}, \\ C_2(0) &= c_2(0) \end{aligned} \quad (\text{B18})$$

and obtain

$$\dot{c}_2(t) = \frac{\sqrt{8\kappa_{p,e1}}\alpha_{in}^2}{i(E_1 - E_0 - i\kappa_p)} [e^{i(E_2 - E_0 - 2i\kappa_p)t} - e^{i(E_2 - E_1 - i\kappa_p)t}]. \quad (\text{B19})$$

Integrating both sides of Eq. (B19), we have

$$\begin{aligned} c_2(t) &= c_2(0) + \frac{\sqrt{8\kappa_{p,e1}}\alpha_{in}^2}{i(E_1 - E_0 - i\kappa_p)} \\ &\times \left[ \frac{e^{i(E_2 - E_0 - 2i\kappa_p)t} - 1}{i(E_2 - E_0 - 2i\kappa_p)} - \frac{e^{i(E_2 - E_1 - i\kappa_p)t} - 1}{i(E_2 - E_1 - i\kappa_p)} \right], \end{aligned} \quad (\text{B20a})$$

$$\begin{aligned} C_2(t) &= c_2(0)e^{-i(E_2 - 2i\kappa_p)t} \\ &+ \frac{\sqrt{8\kappa_{p,e1}}\alpha_{in}^2}{i(E_1 - E_0 - i\kappa_p)} \frac{e^{-iE_0t} - e^{-i(E_2 - 2i\kappa_p)t}}{i(E_2 - E_0 - 2i\kappa_p)} \\ &- \frac{\sqrt{8\kappa_{p,e1}}\alpha_{in}^2}{i(E_1 - E_0 - i\kappa_p)} \frac{e^{-i(E_1 - i\kappa_p)t} - e^{-i(E_2 - 2i\kappa_p)t}}{i(E_2 - E_1 - i\kappa_p)}. \end{aligned} \quad (\text{B20b})$$

According to the initial condition  $c_2(0) = 0$ , we can obtain

$$C_2(t) = \frac{\sqrt{8\kappa_{p,e1}}\alpha_{in}^2}{i(E_1 - E_0 - i\kappa_p)} \left[ \frac{e^{-iE_0t} - e^{-i(E_2 - 2i\kappa_p)t}}{i(E_2 - E_0 - 2i\kappa_p)} \right]. \quad (\text{B21})$$

Therefore, for the infinite-time limit  $t \rightarrow \infty$ , we have

$$\begin{aligned} C_0(\infty) &\equiv C_0 = 1, \\ C_1(\infty) &\equiv C_1 = \frac{\sqrt{2\kappa_{p,e1}}\alpha_{in}}{i(\Delta_p + \delta\omega_{VIC} - i\kappa_p)}, \\ C_2(\infty) &\equiv C_2 = \frac{\sqrt{\kappa_{p,e1}}\alpha_{in}}{i(\Delta_p + \delta\omega_{VIC} + \eta_{VIC} - i\kappa_p)} C_1. \end{aligned} \quad (\text{B22})$$

From Eqs. (B22) we can easily obtain the photon-number fluctuation of the probe field

$$\begin{aligned} \Delta N_a &= \sqrt{\langle (\hat{a}^\dagger \hat{a})^2 \rangle - \langle \hat{a}^\dagger \hat{a} \rangle^2} \\ &\approx |C_1| = \sqrt{\frac{2\kappa_{p,e1}\alpha_{in}^2}{(\Delta_p + \delta\omega_{VIC})^2 + \kappa_p^2}}. \end{aligned} \quad (\text{B23})$$

The statistical properties of the outgoing photon can be evaluated with the steady-state second-order correlation function at zero delay

$$g^{(2)}(0) = \frac{\langle \hat{a}_{out}^\dagger(t) \hat{a}_{out}^\dagger(t) \hat{a}_{out}(t) \hat{a}_{out}(t) \rangle_{SS}}{\langle \hat{a}_{out}^\dagger(t) \hat{a}_{out}(t) \rangle_{SS}^2}, \quad (\text{B24})$$

where  $\hat{a}_{\text{out}} = \sqrt{2\kappa_{p,e2}}\hat{a}$  [46]. Therefore, we have

$$\begin{aligned} g^{(2)}(0) &= \frac{\langle \hat{a}_{\text{out}}^\dagger(t)\hat{a}_{\text{out}}^\dagger(t)\hat{a}_{\text{out}}(t)\hat{a}_{\text{out}}(t) \rangle_{\text{SS}}}{\langle \hat{a}_{\text{out}}^\dagger(t)\hat{a}_{\text{out}}(t) \rangle_{\text{SS}}^2} \\ &= \frac{\langle \hat{a}^\dagger(t)\hat{a}^\dagger(t)\hat{a}(t)\hat{a}(t) \rangle_{\text{SS}}}{\langle \hat{a}^\dagger(t)\hat{a}(t) \rangle_{\text{SS}}^2}. \end{aligned} \quad (\text{B25})$$

This means that the output photon mode has the same statistical properties as that in the probe cavity. When  $t \rightarrow \infty$ , substituting Eqs. (B22) and (B3) into Eq. (B25), we obtain

$$g^{(2)}(0) \approx \frac{2|C_2|^2}{|C_1|^4} = \frac{(\Delta_p + \delta\omega_{\text{VIC}})^2 + \kappa_p^2}{(\Delta_p + \delta\omega_{\text{VIC}} + \eta_{\text{VIC}})^2 + \kappa_p^2}, \quad (\text{B26})$$

where  $\delta\omega_{\text{VIC}}$  can be neglected in the case of two-photon resonance in which  $\Delta_{21} = \Delta_{23}$ . When the probe frequency resonates with the cavity, i.e.,  $\Delta_p = 0$ , we get

$$g^{(2)}(0) \approx \frac{2|C_2|^2}{|C_1|^4} = \frac{\kappa_p^2}{\eta_{\text{VIC}}^2 + \kappa_p^2}. \quad (\text{B27})$$

The second-order correlation function  $g^{(2)}(0)$  measures the statistical properties of the quantum average of the system. Thus, for the CFC configuration, we can replace the quantum nonlinear coefficient  $\eta_{\text{VIC}}$  by  $\eta_{\text{CFC}} = \langle \hat{\eta}_{\text{CFC}} \rangle$  to obtain the approximate function

$$g^{(2)}(0) \approx \frac{(\Delta_p + \delta\omega_{\text{CFC}})^2 + \kappa_p^2}{(\Delta_p + \delta\omega_{\text{CFC}} + \eta_{\text{CFC}})^2 + \kappa_p^2}. \quad (\text{B28})$$

Now we calculate the fluctuation  $\Delta G$  of the second-order correlation operator [3,41]  $\hat{G} = \hat{a}_{\text{out}}^\dagger\hat{a}_{\text{out}}^\dagger\hat{a}_{\text{out}}\hat{a}_{\text{out}}$  in the case of  $\Delta_p = 0$ . In the VIC configuration, we have

$$\begin{aligned} \Delta G_{\text{VIC}} &= \sqrt{\langle \hat{G}_{\text{VIC}}^2 \rangle - \langle \hat{G}_{\text{VIC}} \rangle^2} \\ &= (2\kappa_{p,e2})^2 \sqrt{\langle (\hat{a}^\dagger\hat{a}^\dagger\hat{a}\hat{a})^2 \rangle - \langle \hat{a}^\dagger\hat{a}^\dagger\hat{a}\hat{a} \rangle^2} \\ &\approx 2(2\kappa_{p,e2})^2 |C_2| \\ &\approx \frac{8\sqrt{2}\kappa_{p,e1}\kappa_{p,e2}^2\alpha_{\text{in}}^2}{\kappa_p\sqrt{\eta_{\text{VIC}}^2 + \kappa_p^2}}. \end{aligned} \quad (\text{B29})$$

For a strong nonlinearity, i.e.,  $\eta_{\text{VIC}} \gg \kappa_p$ , Eq. (B29) becomes

$$\Delta G_{\text{VIC}} \approx \frac{8\sqrt{2}\kappa_{p,e1}\kappa_{p,e2}^2\alpha_{\text{in}}^2}{\kappa_p\eta_{\text{VIC}}}. \quad (\text{B30})$$

Similarly, we can obtain the fluctuation

$$\Delta G_{\text{CFC}} \approx \frac{8\sqrt{2}\kappa_{p,e1}\kappa_{p,e2}^2\alpha_{\text{in}}^2}{\kappa_p\eta_{\text{CFC}}}. \quad (\text{B31})$$

for the CFC configuration. Substituting Eqs. (A24) into Eq. (B31), we get

$$\Delta G_{\text{CFC}} \approx \frac{8\sqrt{2}\kappa_{p,e1}\kappa_{p,e2}^2\alpha_{\text{in}}^2}{\bar{\eta}_{\text{CFC}}\kappa_p} + \frac{8\sqrt{2}\kappa_{p,e1}\kappa_{p,e2}^2\alpha_{\text{in}}^2}{\bar{\eta}_{\text{CFC}}\kappa_p} \left( \frac{\Delta N_c}{N_c} \right)^2. \quad (\text{B32})$$

- 
- [1] A. Di Piazza, C. Müller, K. Z. Hatsagortsyan, and C. H. Keitel, Extremely high-intensity laser interactions with fundamental quantum systems, *Rev. Mod. Phys.* **84**, 1177 (2012).
- [2] M. O. Scully and M. S. Zubairy, *Quantum Optics*, 3rd ed. (Cambridge University Press, Cambridge, 1997).
- [3] D. F. Walls and G. J. Milburn, *Quantum Optics*, 2nd ed. (Springer Science + Business Media, Berlin, 2007).
- [4] I. M. Georgescu, S. Ashhab, and F. Nori, Quantum simulation, *Rev. Mod. Phys.* **86**, 153 (2014).
- [5] H. M. Wiseman and G. J. Milburn, *Quantum Measurement and Control* (Cambridge University Press, Cambridge, 2009).
- [6] A. A. Clerk, M. H. Devoret, S. M. Girvin, F. Marquardt, and R. J. Schoelkopf, Introduction to quantum noise, measurement, and amplification, *Rev. Mod. Phys.* **82**, 1155 (2010).
- [7] G. Brida, M. Genovese, and I. Ruo Berchera, Experimental realization of sub-shot-noise quantum imaging, *Nat. Photon.* **4**, 227 (2010).
- [8] J. A. Souza, E. Figueroa, H. Chibani, C. J. Villas-Boas, and G. Rempe, Coherent Control of Quantum Fluctuations Using Cavity Electromagnetically Induced Transparency, *Phys. Rev. Lett.* **111**, 113602 (2013).
- [9] D. Zhao, All-optical active control of photon correlations: Dressed-state-assisted quantum interference effects, *Phys. Rev. A* **98**, 033834 (2018).
- [10] P. A. M. Dirac, The quantum theory of the emission and absorption of radiation, *Proc. R. Soc. London Ser. A* **114**, 243 (1927).
- [11] F. J. Garcia-Vidal, C. Ciuti, and T. W. Ebbesen, Manipulating matter by strong coupling to vacuum fields, *Science* **373**, eabd0336 (2021).
- [12] T. Yoshie, A. Scherer, J. Hendrickson, G. Khitrova, H. M. Gibbs, G. Rupper, C. Ell, O. B. Shchekin, and D. G. Deppe, Vacuum Rabi splitting with a single quantum dot in a photonic crystal nanocavity, *Nature (London)* **432**, 200 (2004).
- [13] H. Tanji-Suzuki, W. Chen, R. Landig, J. Simon, and V. Vuletić, Vacuum-induced transparency, *Science* **333**, 1266 (2011).
- [14] W. Guerin, T. S. d. E. Santo, P. Weiss, A. Cipris, J. Schachenmayer, R. Kaiser, and R. Bachelard, Collective Multimode Vacuum Rabi Splitting, *Phys. Rev. Lett.* **123**, 243401 (2019).
- [15] W. Dittrich and H. Gies, in *Probing the Quantum Vacuum: Perturbative Effective Action Approach in Quantum Electrodynamics and its Application*, edited by J. Kühn, T. Müller, A. Ruckenstein, F. Steiner, J. Trümper, and P. Wölffe, Springer Tracts in Modern Physics Vol. 166 (Springer Science + Business Media, New York, 2000).
- [16] B. King, A. Di Piazza, and C. H. Keitel, A matterless double slit, *Nat. Photon.* **4**, 92 (2010).
- [17] H. B. G. Casimir, On the attraction between two perfectly conducting plates, *Proc. K. Ned. Akad. Wet. B* **51**, 793 (1948).
- [18] K. Y. Fong, H.-K. Li, R. Zhao, S. Yang, Y. Wang, and X. Zhang, Phonon heat transfer across a vacuum through quantum fluctuations, *Nature (London)* **576**, 243 (2019).

- [19] E. M. Purcell, *Confined Electrons and Photons* (Springer, Boston, 1995), pp. 839–839.
- [20] J. M. Raimond, M. Brune, and S. Haroche, Manipulating quantum entanglement with atoms and photons in a cavity, *Rev. Mod. Phys.* **73**, 565 (2001).
- [21] A. Reiserer and G. Rempe, Cavity-based quantum networks with single atoms and optical photons, *Rev. Mod. Phys.* **87**, 1379 (2015).
- [22] A. A. Abdumalikov, Jr., O. Astafiev, Y. Nakamura, Y. A. Pashkin, and J. Tsai, Vacuum Rabi splitting due to strong coupling of a flux qubit and a coplanar-waveguide resonator, *Phys. Rev. B* **78**, 180502(R) (2008).
- [23] H. Toida, T. Nakajima, and S. Komiyama, Vacuum Rabi Splitting in a Semiconductor Circuit QED System, *Phys. Rev. Lett.* **110**, 066802 (2013).
- [24] K. Santhosh, O. Bitton, L. Chuntonov, and G. Haran, Vacuum Rabi splitting in a plasmonic cavity at the single quantum emitter limit, *Nat. Commun.* **7**, ncomms11823 (2016).
- [25] J.-S. Tang, W. Nie, L. Tang, M. Chen, X. Su, Y. Lu, F. Nori, and K. Xia, Nonreciprocal Single-Photon Band Structure, *Phys. Rev. Lett.* **128**, 203602 (2022).
- [26] A. Imamoglu, H. Schmidt, G. Woods, and M. Deutsch, Strongly Interacting Photons in a Nonlinear Cavity, *Phys. Rev. Lett.* **79**, 1467 (1997).
- [27] D. E. Chang, V. Vuletić, and M. D. Lukin, Quantum nonlinear optics—photon by photon, *Nat. Photon.* **8**, 685 (2014).
- [28] D. Vitali, M. Fortunato, and P. Tombesi, Complete Quantum Teleportation with a Kerr Nonlinearity, *Phys. Rev. Lett.* **85**, 445 (2000).
- [29] A. Joshi and M. Xiao, Phase gate with a four-level inverted-Y system, *Phys. Rev. A* **72**, 062319 (2005).
- [30] R. Yanagimoto, T. Onodera, E. Ng, L. G. Wright, P. L. McMahon, and H. Mabuchi, Engineering a Kerr-Based Deterministic Cubic Phase Gate via Gaussian Operations, *Phys. Rev. Lett.* **124**, 240503 (2020).
- [31] J. Tang, L. Tang, H. Wu, Y. Wu, H. Sun, H. Zhang, T. Li, Y. Lu, M. Xiao, and K. Xia, Towards On-Demand Heralded Single-Photon Sources via Photon Blockade, *Phys. Rev. Appl.* **15**, 064020 (2021).
- [32] J. Tang, Y. Wu, Z. Wang, H. Sun, L. Tang, H. Zhang, T. Li, Y. Lu, M. Xiao, and K. Xia, Vacuum-induced surface-acoustic-wave phonon blockade, *Phys. Rev. A* **101**, 053802 (2020).
- [33] K. Xia and J. Twamley, All-Optical Switching and Router via the Direct Quantum Control of Coupling between Cavity Modes, *Phys. Rev. X* **3**, 031013 (2013).
- [34] A. Blais, A. L. Grimsmo, S. M. Girvin, and A. Wallraff, Circuit quantum electrodynamics, *Rev. Mod. Phys.* **93**, 025005 (2021).
- [35] A. Noguchi, R. Yamazaki, Y. Tabuchi, and Y. Nakamura, Qubit-Assisted Transduction for a Detection of Surface Acoustic Waves near the Quantum Limit, *Phys. Rev. Lett.* **119**, 180505 (2017).
- [36] S. Rebić, A. S. Parkins, and S. M. Tan, Photon statistics of a single-atom intracavity system involving electromagnetically induced transparency, *Phys. Rev. A* **65**, 063804 (2002).
- [37] H. Kang and Y. Zhu, Observation of Large Kerr Nonlinearity at Low Light Intensities, *Phys. Rev. Lett.* **91**, 093601 (2003).
- [38] H. Zheng, D. J. Gauthier, and H. U. Baranger, Cavity-Free Photon Blockade Induced by Many-Body Bound States, *Phys. Rev. Lett.* **107**, 223601 (2011).
- [39] C. Hamsen, K. N. Tolazzi, T. Wilk, and G. Rempe, Strong coupling between photons of two light fields mediated by one atom, *Nat. Phys.* **14**, 885 (2018).
- [40] H.-P. Breuer and F. Petruccione, *The Theory of Open Quantum Systems* (Oxford University Press, New York, 2002).
- [41] S. Ghosh and T. C. H. Liew, Dynamical Blockade in a Single-Mode Bosonic System, *Phys. Rev. Lett.* **123**, 013602 (2019).
- [42] J. R. Johansson, P. D. Nation, and F. Nori, QuTiP: An open-source Python framework for the dynamics of open quantum systems, *Comput. Phys. Commun.* **183**, 1760 (2012).
- [43] Y.-Q. Li and M. Xiao, Electromagnetically induced transparency in a three-level  $\Lambda$ -type system in rubidium atoms, *Phys. Rev. A* **51**, R2703 (1995).
- [44] J. Sheng, X. Yang, H. Wu, and M. Xiao, Modified self-Kerr nonlinearity in a four-level N-type atomic system, *Phys. Rev. A* **84**, 053820 (2011).
- [45] K. Xia, F. Nori, and M. Xiao, Cavity-Free Optical Isolators and Circulators Using a Chiral Cross-Kerr Nonlinearity, *Phys. Rev. Lett.* **121**, 203602 (2018).
- [46] C. W. Gardiner and M. J. Collett, Input and output in damped quantum systems: Quantum stochastic differential equations and the master equation, *Phys. Rev. A* **31**, 3761 (1985).
- [47] R. Huang, A. Miranowicz, J.-Q. Liao, F. Nori, and H. Jing, Nonreciprocal Photon Blockade, *Phys. Rev. Lett.* **121**, 153601 (2018).
- [48] X. Su, J.-S. Tang, and K. Xia, Nonlinear dissipation-induced photon blockade, *Phys. Rev. A* **106**, 063707 (2022).